Photovoltaic based dynamic voltage restorer with power saver capability using PI controller

M. Ramasamy [a,*], S. Thangavel [b,1]

[a] Department of Electrical and Electronics Engineering, K.S.R. College of Engineering, Tiruchengode 637 215, Tamil Nadu, India
[b] Department of Electrical and Electronics Engineering, K.S. Rangasamy College of Technology, Tiruchengode 637 215, Tamil Nadu, India

ABSTRACT

In this paper, a photovoltaic (PV) based dynamic voltage restorer (DVR) is proposed to handle deep voltage sags, swells and outages on a low voltage residential distribution system. The PV based DVR can recover sags up to 10%, swells up to 190% of its nominal value. Otherwise, it will operate as an Uninterruptable Power Supply (UPS) when the utility grid fails to supply. It is also designed to reduce the usage of utility grid, which is generated from nuclear and thermal power stations. PV based DVR system is comprised of PV system with low and high power DC–DC boost converter, PWM voltage source inverter, series injection transformer and semiconductor switches. Simulation results proved the capability of the proposed DVR in mitigating the voltage sag, swell and outage in a low voltage distribution system.

© 2011 Elsevier Ltd. All rights reserved.

1. Introduction

Dynamic voltage restorer (DVR) can provide the most cost effective solution to mitigate voltage sags, swells and outages by establishing the proper voltage quality level that is required by sensitive loads. Problems facing industries and residential regarding the power qualities are mainly due to voltage sag, short duration voltage swells and long duration power interruptions [1]. Particularly Tamilnadu, India, has more than 3 h of power interruption in a day. This may occur in developing countries, where the generated electrical power is less than the demand. The above-mentioned power quality problems may disturb the process of production in industries and residences, resulting in equipment damage and loss of revenue.

Voltage sag is a sudden reduction of utility supply voltage which may vary from 90% to 10% of its nominal value. On the other hand, voltage swell is a sudden rise of supply voltage which may vary from 110% to 180% of its nominal value. According to the IEEE 519–1992 and IEEE 1159–1195 standards, a typical duration of voltage sag and swell is 10 ms to 1 min [2]. The outage refers to an interruption of power for long duration. Many research works have been carried out focusing in the design and control of DVR [3–7].

Table 1 shows the voltage variations at Mettur Thermal Power Station (MTPS) in 230 kV bus. From the table, it is observed that there is voltage sag during summer season and voltage swell during winter season. The voltage variation event in 230 kV bus is reflecting on 230 V residential distribution system in the same way. The voltage sags and swells often caused by starting of large induction motors, energizing a large capacitor bank and faults such as single line to ground fault, three phase to ground fault, double line to ground fault on the power distribution system. Voltage sag and swell in power systems produce an important effect on the behavior of sensitive loads. Tripping of power adjustable speed drives (ASD) is one of the greatest voltage sag problems, causing critical loads to stop with the resultant interruption of the manufacturing process several times a year. The resulting loss of time and production, or damaged equipment may cause significant economical losses. To solve the above problems a new method is proposed in this paper.

In general, the voltage injection from DVR compensates the voltage sag, swell and outage. However, it needs a high capacity DC storage system. In the proposed DVR design, a PV system with low and high power DC–DC boost converters are incorporated to function as a high capacity DC voltage source.

Advantages of photovoltaics are:

- Solar power is pollution free.
- Reduced production end wastes and emissions.
- PV installations can operate for many years with little maintenance, so after the initial capital cost of building of any solar power plant, operating costs are extremely low compared to existing power technologies.

* Corresponding author. Mobile: +91 9715614317.
  E-mail addresses: ramasamyksrce@gmail.com (M. Ramasamy), golds71@yahoo.com (S. Thangavel).
  [1] Mobile: +91 9443676688.

Table 1
Voltage variation events in 230 KV bus at MTPS.

Day	Voltage variation in summer (April 2010) in kV		Voltage variation in winter (December 2010) in kV	
	Maximum	Minimum	Maximum	Minimum
1.	227	217	234	226
2.	225	217	233	227
3.	229	222	232	224
4.	227	220	233	227
5.	227	220	233	229
6.	227	219	235	227
7.	228	216	234	227
8.	228	221	233	227
9.	229	220	233	227
10.	229	223	233	226
11.	227	219	233	227
12.	226	214	234	227
13.	228	214	234	225
14.	228	221	233	226
15.	228	223	233	226
16.	228	220	231	225
17.	228	220	231	227
18.	230	224	231	225
19.	230	221	231	229
20.	228	224	233	226
21.	230	223	233	226
22.	230	224	233	227
23.	231	224	234	224
24.	231	226	234	226
25.	231	225	232	224
26.	230	225	231	226
27.	229	223	232	226
28.	230	225	231	225
29.	230	225	231	225
30.	230	225	231	224
31.	–	–	231	225

Disadvantages of photovoltaics are:

- Photovoltaic cells are costly.
- Solar electricity is more expensive than other forms of small scale alternative energy production.

- Solar electricity is not produced at night and is much reduced in cloudy conditions. Therefore, a storage system is required.
- Solar cells produce DC which must be converted to AC.

The location of the proposed PV based DVR in a low voltage single phase distribution system is shown in Fig. 1.

This Paper presents a simulation model of a PV based dynamic voltage restorer capable of handling 10% voltage sags, 190% of voltage swells and outages on a low voltage distribution system. It is also designed to reduce usage of utility power in daytime. In the daytime, DVR will act as online UPS to feed the generated power in PV system to battery and load [8].

2. Proposed DVR

The block diagram of the proposed PV based DVR is shown in Fig. 2. The proposed system mainly consists of a photovoltaic array, low and high power DC/DC boost converters, battery, PWM inverter, series injection transformer, and semiconductor switches S_1, S_2, S_3, R_1 and R_2.

Tables 2 and 3 show the control signals of the semiconductor switches S_1, S_2, S_3 and R_1, R_2 respectively. The power semiconductor switches are controlled by the voltage sensor and logical components.

An injecting transformer is connected in series with the load for restoring sag and swell, and is reconfigured into parallel connection using switches S_1, S_2 and S_3 when handling outage [9]. A DVR can compensate voltage drop across a load by injecting a voltage through a series injection transformer [10]. The injected voltage is in phase with supply voltage, as shown in Fig. 3.

In normal condition, the supply voltage is equal to the load voltage with zero angle. During sag, the supply voltage decreases to a value less than its nominal value. The DVR reacts to the sag event and injects a compensating voltage V_{inj} in phase with the supply voltage to restore the voltage at nominal value. This method is very simple to implement, very fast especially in calculating the DVR compensating voltage. The injected voltage of a DVR (V_{DVR}) can be expressed as

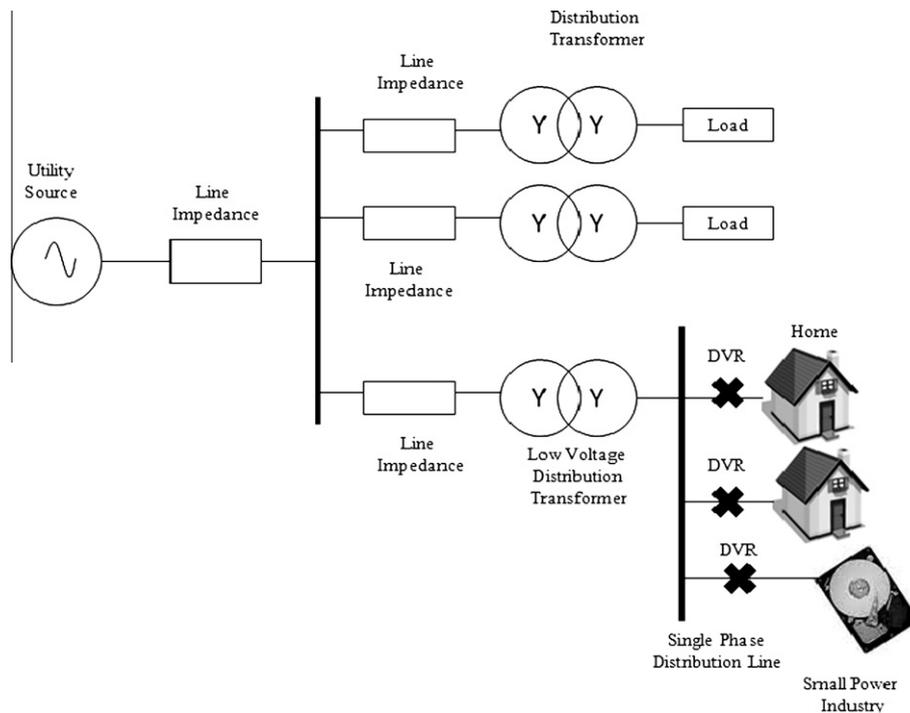$$|V_{inj}| = |V_{presag}| - |V_{sag}| \tag{1}$$

Fig. 1. Typical location of PV based dynamic voltage restorer.

$$V_{\text{DVR}} = V_{inj}$$

$$\angle V_{inj} = \theta_{inj} = \theta_s$$

The inverter is a core component of the DVR. Its control will directly affect the dynamic performance of the DVR. A sinusoidal PWM (SPWM) scheme is used. The carrier waveform is a triangular wave with higher frequency (1080 Hz). The modulation index varies according to the input error signal from the PI controller. The basic idea of SPWM is to compare a sinusoidal control signal of normal frequency 50 Hz with a triangular carrier signal. When the control signal is greater than the carrier signal, the switches turned on and their counter switches are turned off. The output voltage of the inverter mitigates the sag, swell and outage. The DC voltage might be used from PV array if available. Otherwise, the line voltage is rectified and the DC energy is stored in batteries.

3. Photovoltaic array modeling

PV array is a system which uses two or more solar panels to convert sunlight into electricity. PV array is a linked collection of solar cells. The use of new efficient photovoltaic solar cells has emerged as an alternative source of renewable green energy conversion [11,12]. In the proposed DVR, PV array provides a DC source for the DVR. The electrical system powered by solar array requires DC/DC converter due to varying nature of the generated solar power resulting from sudden changes in weather conditions which change the solar irradiation level as well as cell operating temperature. Solar arrays are built up with combined parallel/series combination of solar cells. The PV array is designed and modeled with a low step up boost converter to charge the batteries. An equivalent circuit model of photovoltaic cell is shown in Fig. 4.

The PV model is developed using basic equations of photovoltaic cells including the effects of temperature changes and solar irradiation [13–15]. The PV cell output voltage is a function of the photo current that mainly determined by load current depending on the solar irradiation level during the operation. The solar cell output voltage is shown in Eq. (2).

$$V_c = \frac{AkT_c}{e} \ln\left(\frac{I_{ph} + I_0 - I_c}{I_0}\right) - R_s I_c \tag{2}$$

where V_c is cell output voltage in volts. A is fitting factor. e is electron charge ($1.602 \times 10^{-19} c$). I_{ph} is Photo current (10 A). I_0 is reverse saturation current of diode (0.0002 A). k is Boltzmann constant (1.38×10^{-22} J/°k). I_c is cell output current in A. R_s is solar cell internal resistance (0.001 Ω). T_c is operating temperature of the reference cell (40 °C).

When the irradiation and ambient temperature change, the solar cell operating temperature also changes, resulting in a new output voltage and a new photo current. The solar cell operating temperature varies as a function of solar irradiation level and ambient temperature. The effect of temperature variations are represented in the model by the temperature coefficients C_{TV} and C_{TI}.
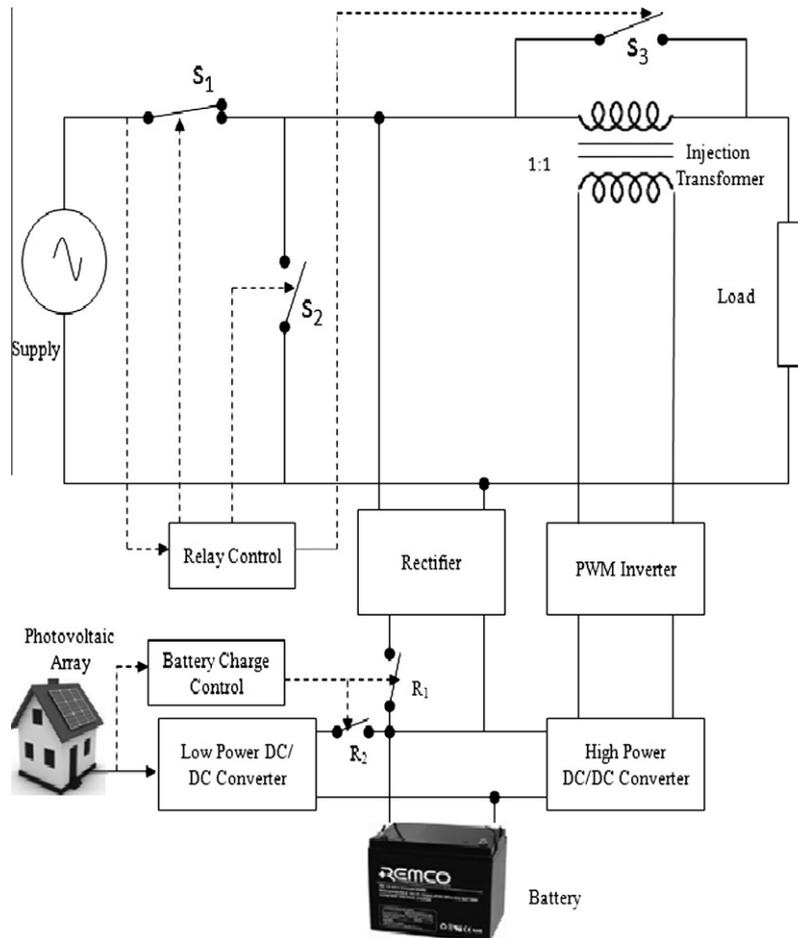

Fig. 2. Block diagram of the proposed PV based DVR.

Table 2
Control signals for S_1, S_2 and S_3.

Supply voltage (%)	Control signals			Mode of operation
	S_1	S_2	S_3	
100	1	0	1	Ideal
<100	1	0	0	DVR
>100	1	0	0	DVR
0	0	1	0	UPS

Table 3
Battery charge control.

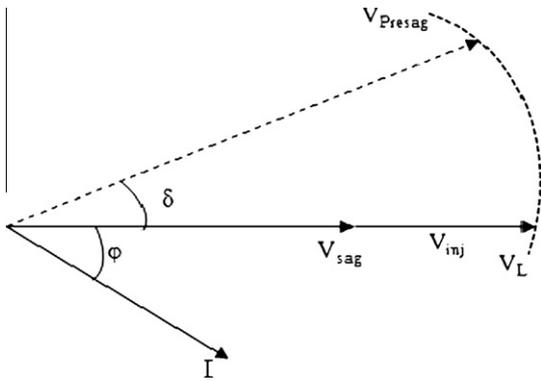| PV voltage (V)	Control signals		Battery charging unit
	R_1	R_2	
>6	0	1	PV array
<6	1	0	Rectifier

Fig. 3. In-phase compensation.

$$C_{TV} = 1 + \beta_T(T_a - T_x) \tag{3}$$

$$C_{TI} = 1 + \frac{\gamma_T}{S_c}(T_a - T_x) \tag{4}$$

where $\beta_T = 0.004$ and $\gamma_T = 0.006$ for the cell used and $T_a = 40\,°C$ is the reference ambient temperature. T_x is atmospheric ambient temperature. The change in the photocurrent and operating temperature due to variation in the solar level can be expressed as follows.

$$C_{SV} = 1 + \beta_T \alpha_s(S_x - S_C) \tag{5}$$

$$C_{SI} = 1 + \frac{1}{S_c}(S_x - S_c) \tag{6}$$

where S_c is reference solar irradiation level ($100\,W/m^3$). S_x is new level of solar irradiation. The new value of cell output voltage and photo current can be expressed as follows.
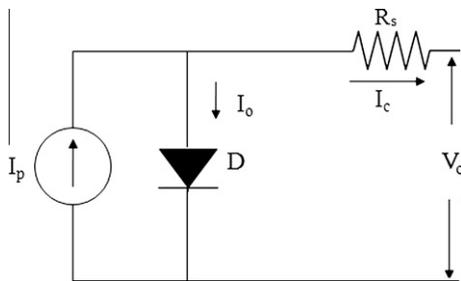

Fig. 4. Equivalent circuit of photovoltaic cell.

$$V_{CX} = C_{TV}C_{SV}V_C \tag{7}$$

$$I_{phx} = C_{TI}C_{SI}I_{ph} \tag{8}$$

The temperature change, ΔT_c, occurs due to the change in solar irradiation level.

$$\Delta T_c = \alpha_s(S_x - S_c)$$

A functional block diagram of photovoltaic (PV) array is shown in Fig. 5. The mathematical model of a single PV cell given by Eq. (2) is represented with the block called *Block 1*. The effect of change in solar irradiation and temperatures are represented in the block called *Block 2*.

Table 4 shows the temperature and solar radiation variations at erode district for the period of 1 month. These data are collected from the Tamil Nadu Agricultural University (TNAU), Coimbatore [16] to estimate the possible output voltage of the PV array with change in temperature and radiation level. From the table and Eq. (7), it is observed that the PV array output voltage may vary between 11.33 V and 6.50 V.

4. DC/DC converter

A DC–DC converter is an electronic circuit to convert a source of DC voltage from one level to another level. Additionally, the battery voltage declines as its stored power is drained. Switched DC–DC converters offer a method to increase voltage from a partially lowered battery voltage thereby saving space instead of using multiple batteries to accomplish the same thing and it regulates the DC voltage.

4.1. Low power DC–DC boost converter

In the boost converter, the output voltage is greater than the input voltage [17]. A low step up DC–DC converter is shown in Fig. 6. Its main function is to regulate the output voltage of the PV array.

The circuit operation can be divided into two modes.

(1) *Mode 1*: When the switch S is on, the diode D_m is reverse biased by switch and V_c, thus isolating the output stage. The input current (i_s), which raises, flows through inductor L and switch S. The input V_s supplies energy to the inductor during on period (T_{on}). The voltage across the inductor (L) in mode 1 is shown in Eq. (9).

$$V_L = L\frac{di_s}{dt} \tag{9}$$

$$V_s = V_L$$

(2) *Mode 2*: When the switch S is off, the inductor current is forced to flow through the diode D_m and load for a period T_{off}. As the current tends to decrease, polarity of the emf induced in inductor L is reversed and it is connected in series with voltage source V_s and load through diode D_m. The output voltage V_o in mode 2 is expressed in Eq. (10).

$$V_0 = V_s + L\frac{di_s}{dt} \tag{10}$$

The average output voltage of the converter is depicted in Eq. (11).

$$V_0 = \frac{V_s}{1 - D} \tag{11}$$

$$D = \frac{T_{on}}{T_{on} + T_{off}}$$

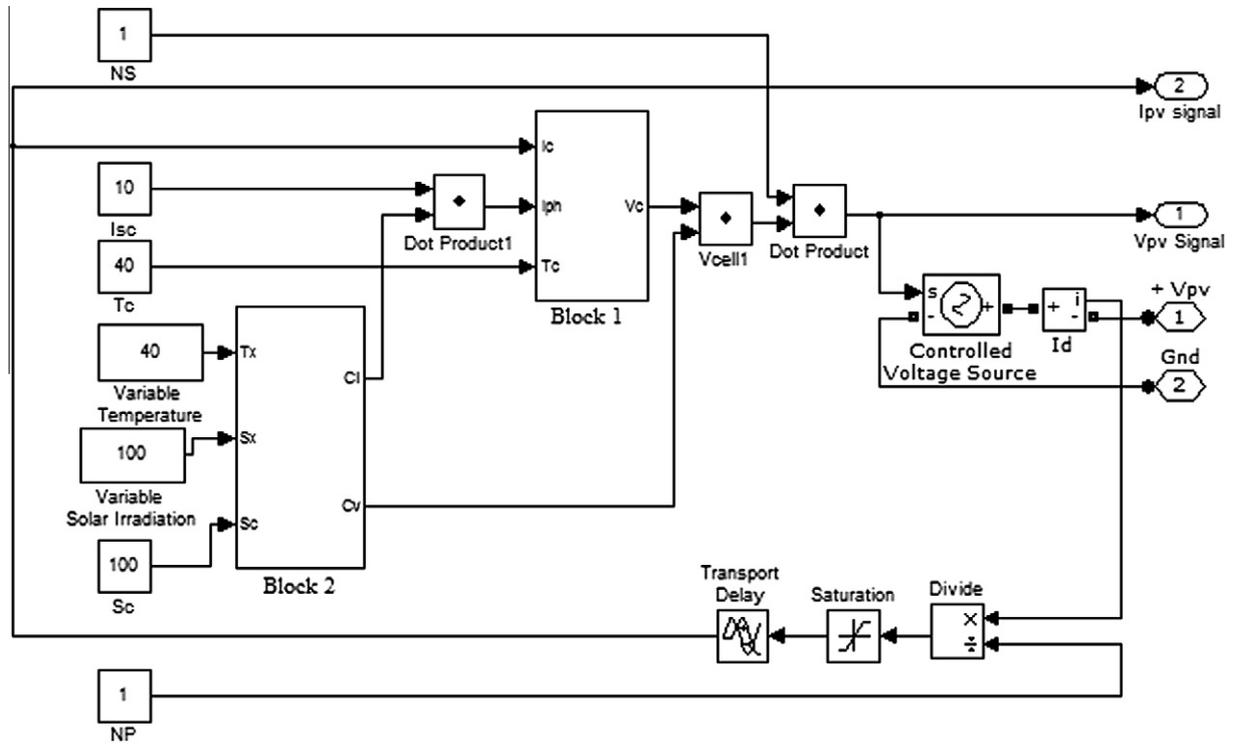where D is duty cycle, T_{on} is on time and T_{off} is off time.

Fig. 5. Functional block diagram of photovoltaic array.

Table 4
Erode district weather data.

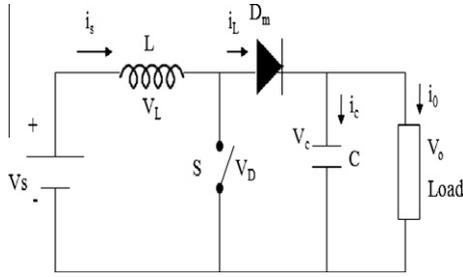| Date	Temperature (°C)		Relative humidity (%)	Rainfall (mm)	Solar radiation (Cal/cm^2)
	Max.	Min.			
01.09.2011	33.2	24.7	70.8	00.0	448.19
02.09.2011	30.9	24.2	79.9	00.0	354.31
03.09.2011	33.5	24.5	77.0	00.0	320.66
04.09.2011	32.6	24.3	72.2	00.0	464.30
05.09.2011	34.1	24.6	71.1	00.0	482.00
06.09.2011	35.3	25.5	68.1	00.0	539.02
07.09.2011	34.7	25.0	66.2	00.0	426.76
08.09.2011	34.3	24.2	68.2	00.0	447.04
09.09.2011	35.5	24.7	70.3	00.5	454.96
10.09.2011	34.6	24.3	68.2	00.0	484.29
11.09.2011	35.5	23.9	76.3	02.0	439.79
12.09.2011	34.1	23.9	73.7	00.0	494.11
13.09.2011	34.7	23.7	72.6	00.0	461.49
14.09.2011	34.8	24.2	71.3	00.0	485.35
15.09.2011	34.6	24.9	67.3	00.0	493.85
16.09.2011	34.3	23.8	71.8	01.0	472.30
17.09.2011	34.9	24.9	71.8	01.5	500.68
18.09.2011	34.3	23.0	67.3	00.0	463.91
19.09.2011	36.3	25.1	62.1	00.0	524.86
20.09.2011	35.4	24.9	65.9	04.0	473.64
21.09.2011	31.3	23.1	74.6	00.0	226.03
22.09.2011	35.7	23.2	67.3	00.0	554.83
23.09.2011	35.1	22.2	66.3	00.0	487.98
24.09.2011	33.9	23.0	63.3	00.0	448.58
25.09.2011	35.8	24.1	59.9	00.0	570.24
26.09.2011	36.0	24.5	59.6	00.5	558.42
27.09.2011	36.4	24.5	64.2	01.0	538.82
28.09.2011	36.2	25.1	57.5	00.0	551.47
29.09.2011	36.6	23.8	61.4	00.0	518.03
30.09.2011	37.1	24.5	64.0	01.5	529.80
Month average	34.7	24.2	68.3	00.5	473.86

Fig. 6. Circuit diagram of low step up DC–DC converter.

4.2. High power DC–DC boost converter

The output voltage level of the low power DC–DC converter and batteries are low. Hence, it is not sufficient to inject the required amount of voltage to load to mitigate voltage sags, swells and outages. For that a high step up DC–DC converter is used to step up the low power dc to high power DC. It is connected in between batteries and PWM voltage source inverter.

The advantages of this converter are:

- High step up gain.
- Voltage Stress across the switch is low.
- It has low conduction loss.
- Coupled inductor coil is less than other coupled inductor converters.
- High efficiency.

Fig. 7 shows the circuit diagram of high step up DC–DC converter [18–21].

The main operating principle of this converter is that when the switch S is turned on, the coupled inductor induces voltage on the secondary side and magnetic inductor L_m is charged by V_{in}. The induced voltage in the secondary makes V_{in}, V_{C1}, V_{C2} and V_{C3} to release energy to the load in series. When the switch S is turned off, the energy stored in the magnetic inductor L_m is released via secondary side of coupled inductor to charge the capacitors C_2 and C_3 in parallel. The proposed converter operation can be divided into five mode of operation [18]. The output equation of high step up DC–DC converter is shown in Eq. (12).

$$V_0 = V_{in} + V_{c1} + V_{c2} + V_{L2}^{II} + V_{c3} \tag{12}$$

where V_{C1} is voltage across the capacitor C_1 in voltage. V_{C2} in voltage across the capacitor C_2 in voltage. V_{C3} is voltage across the capacitor

C_3 in voltage. V_{L2}^{II} is voltage across the secondary of the coupled inductor (N_s) in mode II.

$$V_{L2}^{II} = kV_{in} \tag{13}$$

$$V_{c1} = \frac{D}{1-D} V_{in} \frac{(1+k) + (1-k)n}{2} \tag{14}$$

$$V_{c2} = V_{c3} = \frac{nDk}{1-D} V_{in} \tag{15}$$

where k is coupling coefficient ($k = \frac{L_m}{L_m + L_k}$), n is coupled inductor turns ratio ($\frac{N_s}{N_p}$) and D is duty cycle $D = \frac{T_{on}}{T_{on} + T_{off}}$.or

$$V_0 = V_{in}.M_{CCM} \tag{16}$$

$$M_{CCM} = \frac{1 + n + nD}{1 - D} \tag{17}$$

5. Simulation results and discussion

To illustrate the effectiveness of the PV based DVR for voltage sag, voltage swell and outage mitigation on low voltage single phase distribution system is shown in Fig. 8. A 3 KVA, 230/230 V transformer is used for connecting the DVR to the network. The proposed DVR model is simulated by MATLAB simulink to compensate voltage sag, voltage swell and outages at the source side.

The simulation parameters are shown in Table 5.

The total simulation period is 1 s. Using the facilities available in MATLAB the DVR is simulated to be in operation only when the supply voltage differs from its nominal value. Otherwise, the DVR will act as online ups when the PV array output is greater than 6 V. It reduces the energy consumption from the utility grid. When the PV array generates more power than the load demand, the excess power is stored in the battery. Therefore, during the no injection period, the generated power in the PV array charges the batteries. During the night time, the output voltage of the PV array is too low. At that time, the batteries are charged by the supply.

A programmable three phase voltage source is used to provide the single phase variable voltage at the source end. The first simulation contains no DVR, a reduced voltage (184 V) is applied, during the period 0.1 s to 0.2 s, a raised voltage (276 V) is applied, during the period 0.7 s to 0.8 s and zero voltage (0 V) is applied, during the period 0.3 s to 0.6 s, as presented in Fig. 9a. The voltage sag and swell at the source point is 30%
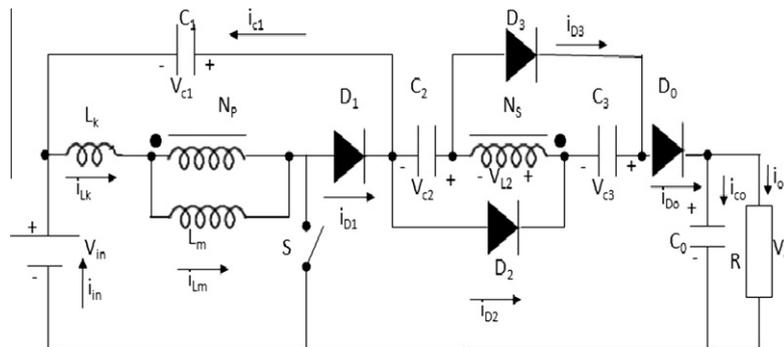

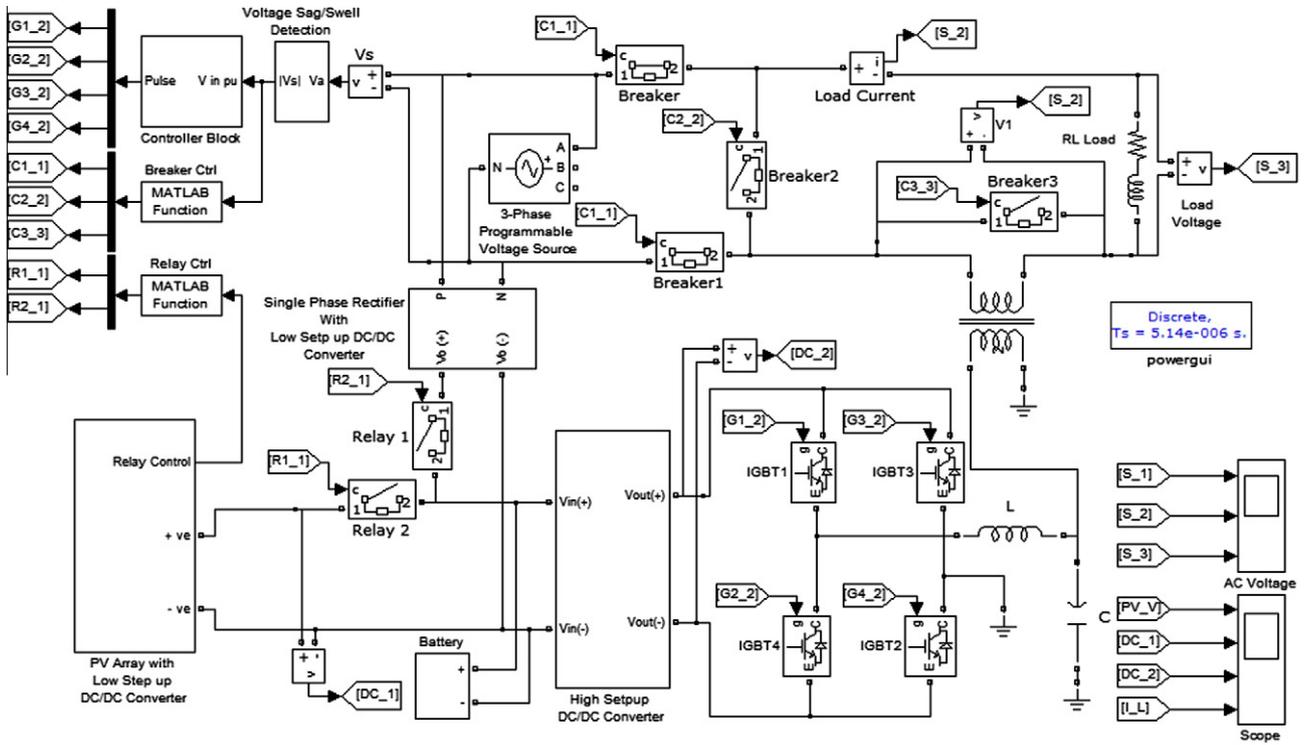**Fig. 7.** High step up DC–DC converter.

Fig. 8. Simulation model of proposed PV based DVR with PI controller.

and 20% with respect to the reference voltage. The injected voltage, load voltage and load current of the DVR are shown in Fig. 9b–d.

The PV array consists of 9 PV cells, all connected in series to have a desired voltage output. Depending on the load power required, the number of parallel branches can be increased to 9 or more [22]. Usually the PV array with boost converter provides increased output voltage with more ripples. However in the proposed method, the presence of LC filter and batteries in the output of the low step up dc-dc converter reduces the ripple and increases the stability of the DC source. Fig. 10a and b shows the PV array voltage without and with boost converter, respectively.

Fig. 11 shows typical characteristics of a PV module with different values of irradiation level with constant temperature (40 °C). The product of the current and voltage represents the output power of the PV array. The maximum power produced by the module is reached at a point on the characteristics where the product of voltage and current is maximum. Two lead acid batteries with 12 V, 88 Ah are connected in series is used to obtain 24 V. The battery parameters are shown in Table 6 [23].

Table 5
Simulation parameters.

Parameters	Values
Load resistance, R_L (Ω)	20
Load inductance (mH)	10
Source voltage (V)	230
Load voltage (V)	230
Rated load current (A)	10

The high power boost converter specifications are:

(1) Input DC voltage V_{in} = 24 V.
(2) Output DC voltage V_o = 230 V.
(3) Maximum output power = 4 KW.
(4) Switching frequency = 25 kHz.
(5) L_m = 48 μH, L_k = 0.25 μH.
(6) C_1 = 3.151 μF/100 V, C_2 = C_3 = 1.062 μF/200 V and C_0 = 500 μF/450 V.

Fig. 12 shows the output voltage of the high power boost converter. The converter is operated in continuous conduction mode (CCM). The steady state analysis of the high step up DC–DC converter is presented in [18]. Under the full load operating condition V_{in} = 24 V, V_0 = 230 V and P_o = 2.3 KW. A control circuit is incorporated with the proposed converter to regulate the output voltage at 230 V.

6. Conclusion

The design of a dynamic voltage restorer (DVR) which incorporates a PV array module with low and high power boost converters as a DC voltage source to mitigate voltage sags, swells and outages in low voltage single phase distribution systems has been presented. The modeling and simulation of the proposed PV based DVR using MATLAB simulink has been presented. The PI controller utilizes the error signal from the comparator to trigger the switches of an inverter using a sinusoidal PWM scheme. The proposed DVR utilizes the energy drawn from the PV array and the utility source during normal operation and stored in batteries and which is converted to an adjustable single phase ac voltage for mitigation of voltage sag, swell and outage. The simulation result shows that the PV based DVR performance is satisfactory in mitigating the voltage variations.

(a) Supply Voltage

(b) Injected Voltage
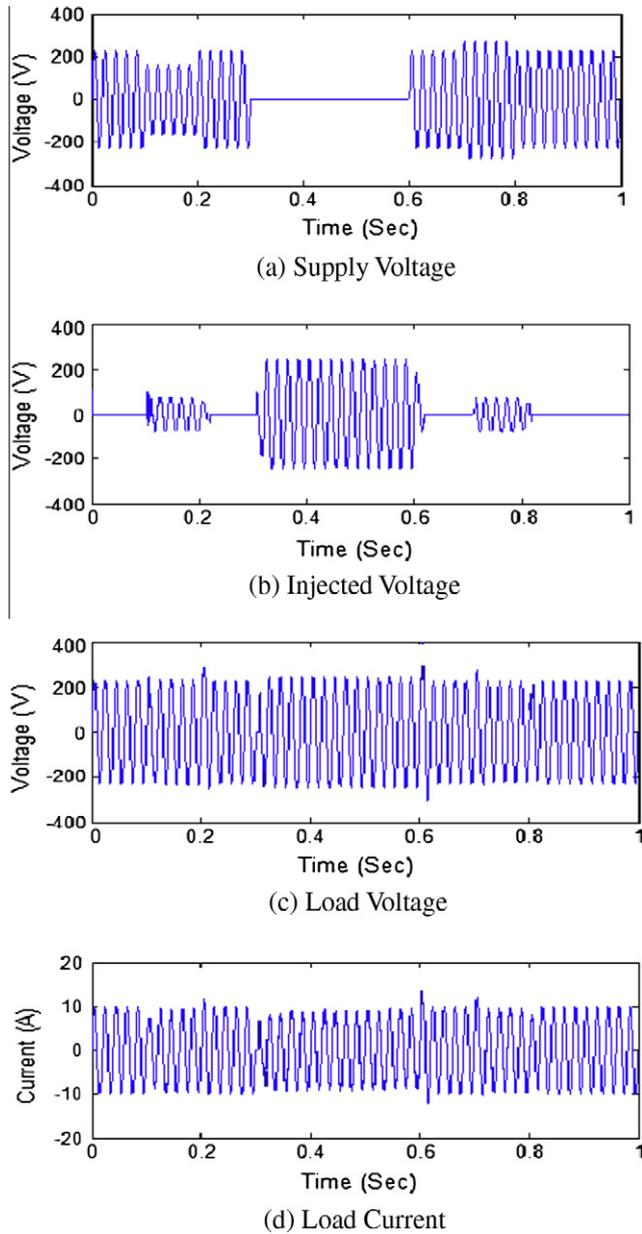

(c) Load Voltage

(d) Load Current

Fig. 9. Supply voltage, injected voltage, load voltage and load current. (a) Supply voltage, (b) injected voltage, (c) load voltage, and (d) load current.

The proposed DVR is operated in:

- Standby mode, where the PV array voltage is zero and the inverter is not active in the circuit to keep the voltage to its nominal value.
- Active mode, where the DVR senses the sag, swell and outage. DVR reacts fast to inject the required single phase compensation voltages.
- Bypass mode, where DVR is disconnected and bypassed in case of maintenance and repair.
- Power saver mode, when the PV array with low power dc-dc converter voltage is enough to handle the load.

Further work will include a comparison with laboratory experiments on a low voltage DVR in order to compare simulation and experimental results. The dynamic performance of the DVR and multiple functions of DVR require further investigation.

(a) PV array output Voltage without low power boost converter

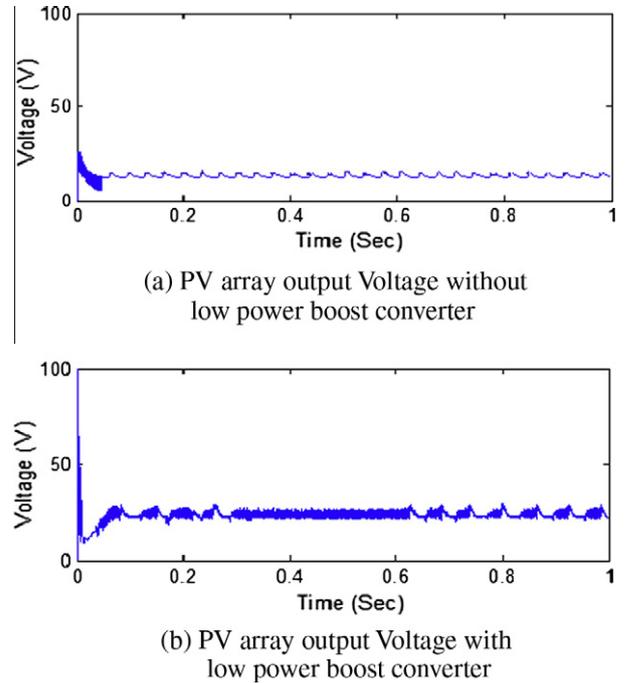(b) PV array output Voltage with low power boost converter

Fig. 10. PV array output voltage without and with boost converter (a) PV array output voltage without low power boost converter and (b) PV array output voltage with low power boost converter.
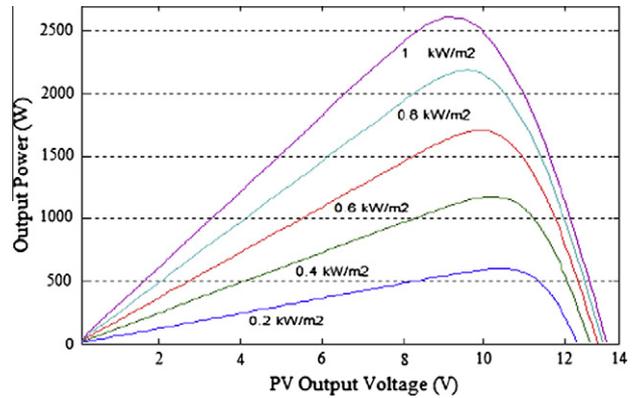

Fig. 11. P–V characteristic of a PV module with different values of irradiance.

Table 6
Battery parameters.

Parameters	Values
Nominal voltage (V)	12
Nominal capacity (Ah)	88
Nominal power (W)	360
Internal resistance (Ω)	0.00136
Nominal discharge current (A)	17.6

Fig. 12. Output voltage of the high step up DC–DC converter.

Acknowledgments

References

[1] Moreno-Munoz A, de-la-rosa JJG, Lopez-Rodriguez MA, Flores-Aries JM, Bellido-Outerino FJ, Ruiz-de-Adana M. Improvement of power quality using distributed generation. In J Electr Power Energy Syst 2010;32(10):1069–76.

[2] Ezoji H, Sheikholeslami A, Tabasi M, Saeednia MM. Simulation of dynamic voltage restorer using hysteresis voltage control. Eur J Sci Res 2009;27(1):152–66.

[3] Amin Hajizadeh, Masoud Aliakbar Golkar. Control of hybrid fuel cell/energy storage distributed generation system against voltage sag. Int J Electr Power Energy Syst 2010;32(5):488–97.

[4] Jowder FAL. Modeling and simulation of different system topologies for dynamic voltage restorer using simulink. In: Proceeding of electrical power and energy conversion systems conference, Sharjah; 10–12 November 2009. p. 1–6.

[5] Strzelecki R, Benysek G. Control strategies and comparison of the dynamic voltage restorer. In: Proceeding of power quality and supply reliability conference, Parnu; 27–29 August 2008. p. 79–82.

[6] Boonchiam P, Mithulananthan N. Understanding of dynamic voltage restorers through MATLAB simulation. Thammasat Int J Sci Tech 2006;11(3):1–6.

[7] Bayinder KC, Teke A, Tumay M. A robust control of dynamic voltage restorer using Fuzzy Logic. In: Proceeding of electrical machines and power electronics conference, Bodrum; 10–12 September 2007. p. 55–60.

[8] Jayasimha S, Kumar TP. Photovoltaic UPS. In: Proceeding of convergent technologies for Asia–Pacific region conference, vol. 4; 15–17 October 2003. p. 1419–23.

[9] Ashari M, Hiyama T, Pujiantara M, Suryoatmojo H, Hery Purnomo M. A Novel dynamic voltage restorer with outage handling capability using fuzzy logic controller. In: Proceeding of innovative computing, information and control conference, Kumamoto; 5–7 September 2007. p. 51.

[10] El-Shennawy TI, Moussa AM, El-Gammal MA, Abou-Ghazala AY. A dynamic voltage restorer for voltage sag mitigation in a refinery with induction motors loads. Am J Eng Appl Sci 2010;3(1):144–51.

[11] Masato Oshiro, Kenichi Tanaka, Tomonobu Seniyu, Shohei Toma, Atsushi Yona, Ashmed Yousuf Saber, et al. Optimal voltage control in distribution systems using PV generators. Int J Electr Power Energy Syst 2011;33(3):485–92.

[12] Habeebullah Sait H, Arual Daniel S. New control paradigm for integration of photovoltaic energy source with utility network. Int J Electr Power Energy Syst 2011;33(1):86–93.

[13] Altas H, Sharaf AM. A photovoltaic array simulation model for MATLAB simulink GUI environment. In: Proceeding of clean electrical power conference, Capri; 21–23 May 2007. p. 341–5.

[14] Buresch M. Photovoltaic energy systems design and installation. New York: McGraw-Hill; 1983.

[15] Salameh ZM, Dagher F. The effect of electrical array configuration on the performance of a PV powered volumetric water pump. IEEE Trans Energy Convers 1990;5:653–8.

[16] Tamil Nadu Agricultural Weather Network. <http://tawn.tnau.ac.in/>. <http://tawn.tnau.ac.in/action?action=lastMonthReport&block=49&district=6>.

[17] Mohan N, Undeland TM, Robbins WP. Power electronics converters, applications and design, 3rd ed. Singapore: Jhon Wiley & Sons (Asia) Pty. Ltd.; 2006.

[18] Hsieh YP, Chen JF, Liang TJ, Yang LS. Novel high set-up DC–DC converter for distributed generation system. IEEE Trans Ind Electron 2011.

[19] Wai RJ, Duan RY. High-efficiency DC/DC converter with high voltage gain. Proce Electr Power Appl Conf 2005;152(4):793–802.

[20] Changchien SK, Liang TJ, Chen JF, Yang LS. Novel high step-up DC–DC converter for fuel cell energy conversion system. IEEE Trans Ind Electron 2007;57(6):2007–17.

[21] Baek JW, Ryoo MH, Kim TJ, Yoo DW, Kim JS. High boost converter using voltage multiplier. In: Proceeding of industrial electronic society conference; 6–10 November 2005. p. 6.

[22] Photovoltaic modules TE1300 data sheet, plan my power, Johannesburg, South Africa. <http://www.planmypower.co.za>.

[23] MPL90-12 data sheet. B&B battery (USA) Inc., Commerce, USA. <http://www.powerstream.com/BB.htm>.